

# CVD Diamond Based Miniature Stirling Cooler

**D. E. Patterson<sup>1</sup>, K. D. Jamison<sup>1</sup>, M. Durrett<sup>1</sup>,  
A. Kashani<sup>2</sup>, and D. Gedeon<sup>3</sup>**

<sup>1</sup>Nanohmics, Inc.

Austin, TX 78741

<sup>2</sup>Atlas Scientific

San Jose, CA 95120

<sup>3</sup>Gedeon Associates

Athens, OH 45701

## ABSTRACT

Nanohmics and its partners are developing a compact Stirling refrigerator to help provide a solution to the growing demand for miniature, high efficiency cooling devices. The refrigerator measures 1 cm x 1 cm x 3 mm and incorporates several novel components that are not found in other previously developed Micro Electromechanical Systems (MEMS) Stirling coolers. This innovative cooler includes the use of high thermal conductivity CVD diamond components for the heat exchange plates and compressor/expansion diaphragms along with a reduced dead space, high heat capacity, and low thermal conductivity regenerator.

The miniature refrigerator is operated by piezoelectric crystal drivers that are internally attached to the two diamond diaphragms. The diaphragms are driven at several kilohertz approximately 90 degrees out of phase with each other to establish the appropriate Stirling refrigeration cycle used in an alpha-design Stirling engine. The working stroke of the cooler diaphragms is approximately 4 microns. In order to improve the coolers' performance, the device is charged to an internal working pressure of 500 kPa.

Modeling of this device indicated that it could theoretically provide a lift of 68 mW with a temperature difference of 20 K between the hot and cold heat exchange faces of the device. Although several device designs are tested, no reproducible cooling effect has been found. Further modeling indicates that parasitic heat losses in these miniature coolers may preclude them from working efficiently.

## INTRODUCTION

The ability to efficiently transport thermal energy for cooling applications in a compact package is in high demand. Many devices operate more efficiently at cool temperatures necessitating costly, heavy, and cumbersome cooling equipment. Presently, devices such as optical and infrared detectors as well as microelectronic processors and other devices with planar substrates are more limited by the mean time between failure (MTBF) of cryocooler systems than by the detector or microprocessor component. In addition, the macroscopic properties of the cooler, such as the electrical

interface, power consumption, and extraneous vibration result in undesirable effects. New developments in microminiaturized systems are enabling the design of highly efficient compact cooling systems. The key figure of merit for these devices is the specific capacity, which is defined as the ratio of the heat dissipation capability to the overall mass of the dissipating device. In the case of microlithographically patterned Micro Electromechanical System (MEMS) components, the size is extremely efficient. For example the unique structural designs of micro-oscillating diaphragms prepared by undercut etching of vapor deposited layers enable large heat transport capabilities relative to the overall size of the devices. In particular, Stirling engine-based devices have shown particular promise as efficient MEMS coolers for integrated circuits and other planar detection arrays compared to their counterparts, thermoelectric coolers (TECs).<sup>1,2,3,4</sup> The premise for the Stirling micro-coolers is the transport of heat between two oscillating membranes that cap a fluid-filled (typically gas) cavity. A low thermally conducting heat exchanger (regenerator) that resides within the cavity absorbs and releases heat from the gas and enables efficient heat flow from the cold top plate (expansion heat exchanger plate) and the bottom (compression heat exchanger plate). A number of methods have been proposed for oscillatory actuation of the membrane layers and a variety of the low thermally conducting heat exchange media have been suggested and tested.

In general, performance of a Stirling engine is optimized when the amplitude of the oscillating membrane is kept low (no unnecessary work in compressing the gas), and is operating at higher frequencies ( $>1$  kHz). Furthermore, thermal exchange in the regenerator is most efficient when the pore size and thermal conductivity of the gas heat exchange media are minimized but allow for relatively unencumbered gas flow and transfer of heat to the media. This is manifested at small Wolmersley numbers and is related to the prevention of unwanted frictional drag of the gas against the exchange media surface. Frictional drag can impart counterproductive energy introduction back into the heat exchange end plate and consequently lower the overall conversion efficiency of the cooling device.

In this work, we introduced several novel materials and a simplified structure to a MEMS-based Stirling engine cryocooler system that would simplify assembly and improve the performance of the devices. In our new design, the silicon heat exchanger (outer) plates and flexible membranes described in previous works are replaced with ultrahigh thermally conductive diamond thin films ( $\sim 10$  W/cm K) using diamond MEMS processing techniques. Furthermore, the regenerator was fabricated from optimum heat exchange materials and designed according to the latest Stirling models.

## MODELING

The Stirling cooler design that is modeled for its performance is shown in Figure 1. The device is made using CVD diamond endplates, a piezoelectric crystal driven CVD diamond diaphragm, and a reduced volume regenerator composed of stainless steel and titanium parts. Sage, from Gedeon Associates, is used for predicting the cooling power of Stirling refrigerators. Similar devices are adapted for the smaller volume diamond coolers developed in this work. The principal findings of the refined models point out that parasitic heat losses quickly overwhelm the smaller cooling systems being built for this project and must be mitigated to fabricate a working MEMS-based (or miniature) Stirling cooler. The main ways to achieve an effective miniature Stirling cooler while minimizing heat losses include (in order of importance):

1. Reducing the working volume of the regenerator
2. Minimizing any heat conduction up the walls of the regenerator
3. Reducing the dead volume of the device
4. Maximizing the stroke and drive frequency of the diaphragm
5. Ensuring that the internal working pressure is high (preferably greater than 500 kPa)
6. Minimizing any internal heating of the device.

In our specific case, the key design parameters were:

- A reduced volume regenerator comprised of:
  - An approximately 0.4 mm diameter cylinder that is 1.1 mm in length contained in an evacuated 10 mm diameter by 1.1 mm cylinder.
  - High heat capacity, low thermal conductivity, high surface area internal regenerator material
  - Vacuum between the interior and exterior walls of the regenerator
- Removal of most of the dead space such that the operating diaphragm fills the entire void between the diaphragm and the regenerator.

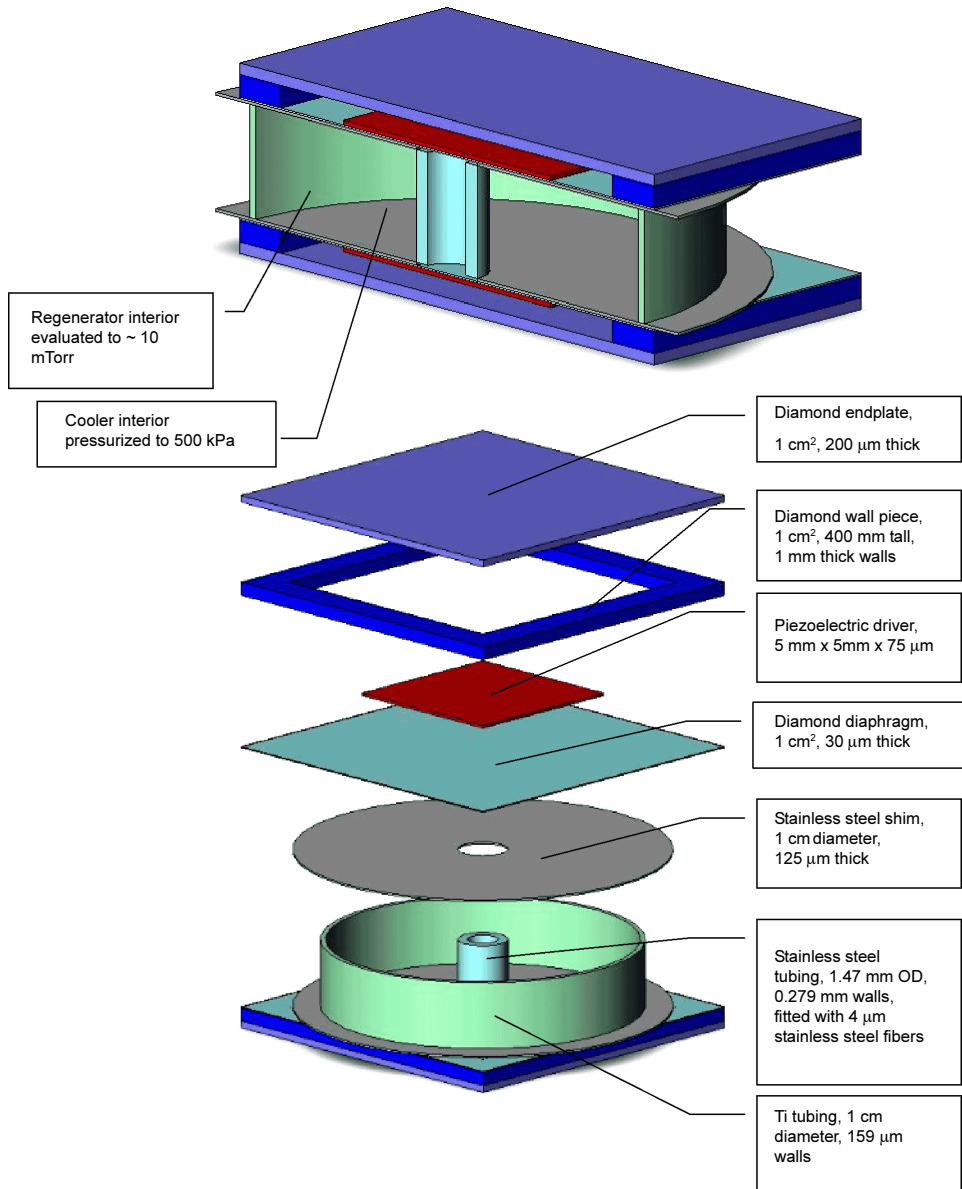


**Figure 1.** Side (top) and Blow-apart (bottom) views of the final prototype diamond-based MEMS cryocooler.

- Maximize diaphragm stroke and frequency without using components that generate excess heat.
- Ensure that the device can be pressurized with a working gas to at least 500 kPa.

Modeling results suggest that a device built to these design parameters would produce a limited amount of lift (68 mW) between a hot endplate temperature of 300 K and a cold endplate temperature of 280 K. Details of the actual device fabrication and performance follow.

## DEVICE FABRICATION

The miniature Stirling cooler is composed of four main parts (endplates, piezoelectric crystal driven diaphragm, regenerator, and evacuation/pressurization ports) that will be described in the next sections.

### CVD Diamond Endplates

All of the CVD diamond components are obtained from Applied Diamond, Inc. of Wilmington, DE. The diamond is produced in an ASTeX 5 kW microwave plasma deposition system and subsequently cut and polished using standard techniques. The endplates are fabricated from two separate pieces of diamond as shown in Figure 2.

The end piece of the endplate is a 1 cm<sup>2</sup> piece of 200  $\mu$ m thick diamond. This piece is not polished, but it is smooth on one side due to growth on a smooth Si template. The smooth face is positioned to be on the outside of the cooler for subsequent attachment to either the device needing cooling or to the ultimate heat sink. The second piece of the endplate is a fully polished 1 cm<sup>2</sup> piece of 400  $\mu$ m thick diamond slab that has the center portion removed by laser trimming. The resultant piece forms the 1 mm walls of the endplate.

The two pieces are joined together with a pre-cut film of Ti/Cu/Ag braze. Extreme care is taken to ensure that the braze does not flow into the central cavity of the endplate. Any residual braze located on the exterior of the endplates is ground off to prevent potential electric shorts in the final device. The finished endplates are shown in Figure 3.

### CVD Diamond Diaphragms and Piezoelectric Crystal Drivers

The CVD diamond diaphragms are also obtained from Applied Diamond, Inc. as cut and polished 1 cm<sup>2</sup> by 30 mm thick pieces. This thickness offers the optimum performance in terms of durability and flexibility. The diaphragms could be deflected to a maximum of 50  $\mu$ m before a rupture of the films. As charging of the devices to their final working pressure of 500-1000 kPa places a tremendous force on the diamond diaphragms, a 50  $\mu$ m hole was laser drilled into each diaphragm to equalize the pressure on both sides of the diaphragm. The effect of this port on the operation of the device is determined following Sharipova.<sup>5</sup> Mathematica<sup>®</sup> is used for the numeri-

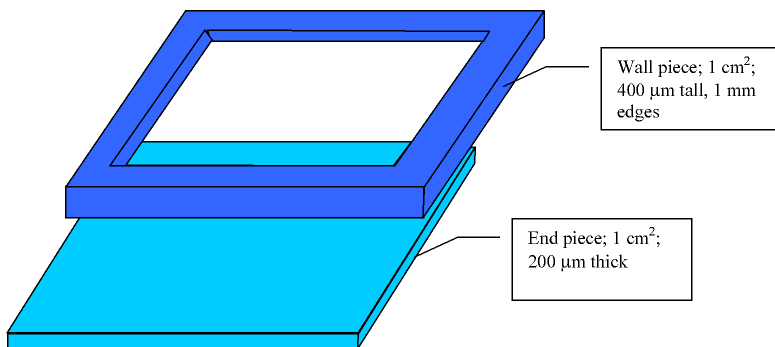


**Figure 2.** Blow-apart view of the endplate. The endplate is fabricated from two separate pieces of diamond that are bonded together.

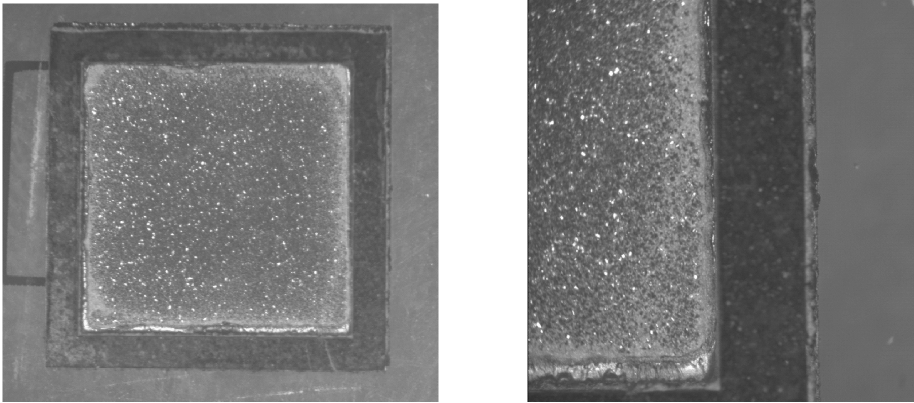


**Figure 3.** Photographs of the assembled  $1\text{ cm}^2 \times 0.6\text{ mm}$  tall CVD diamond endplate. The photograph on the right is a close-up of a corner of the device. The brazing material can be seen to barely extend into the device's well.

cal solution. The calculations indicate that a negligible inefficiency can be expected by placing these pinholes in the diaphragms. A diaphragm with the pressure equalization port is shown in Figure 4.

Several potential driver systems were evaluated for the diamond coolers – piezoelectric, magnetostrictive, electrostatic, and electromagnetic. Piezoelectric drivers were found to offer the best properties of the four candidates in terms of small size, high frequency operation, and good deflection. A lead zirconate titanate (PZT) in an Industry Type 5H, Navy Type IV form (PSI-5H4E; Piezo Systems, Inc.) was ultimately used. The as-supplied  $5\text{ mm} \times 5\text{ mm} \times 0.127\text{ mm}$  thick pieces were further polished down to  $0.060\text{ mm}$  thickness for use in the diamond coolers. The PZT crystals were attached to the center of the diamond diaphragms using silver-filled epoxy (Epo-Tek H22; Epoxy Technologies, Inc.). Thin copper lead wires were then connected to the PZT using the silver epoxy. Finally, the assembled diaphragm was attached to the endplates using a high thermal conductivity, insulating epoxy (Epo-Tek 930-4; Epoxy Technologies, Inc.). The resultant finished endplate pieces are shown in Figure 5.

### Regenerator

The regenerator is a key component in any Stirling cycle device. It must act as a heat storage and heat transfer medium. Therefore, the ideal regenerator has a high heat capacity coupled with a

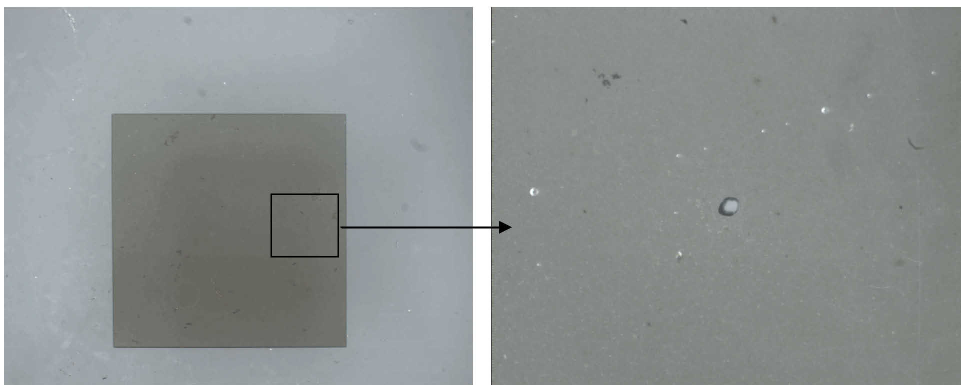


**Figure 4.**  $30\text{ }\mu\text{m}$  thick diamond diaphragm with a  $50\text{ }\mu\text{m}$  pressure equalization port (left) drilled into one side.

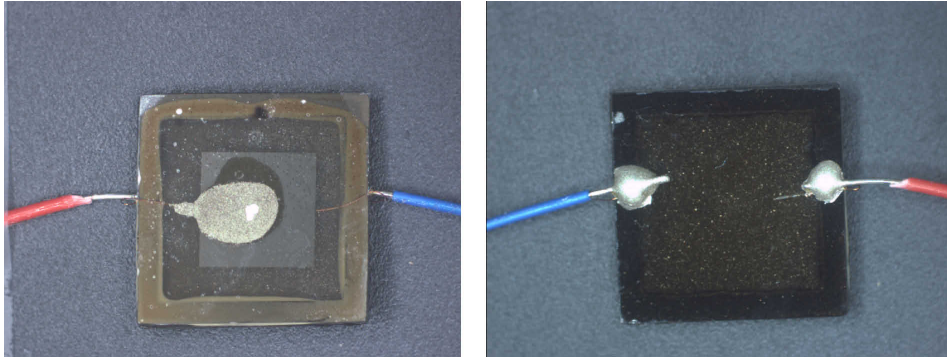


**Figure 5.** Assembled endplate/diaphragm components. The diaphragm side view (right) shows the internal components and the backside view (left) shows the external lead attachment.

low thermal conductivity. Additionally, the regenerator must have a high surface area for maximum gas-to-regenerator contact, yet the device must not restrict gas flow significantly. The regenerator needs to be sufficiently stiff so that it does not act as an additional piston in the cooler, and finally, the regenerator in miniature devices must minimize all dead space, i.e., the diaphragms (pistons) should occupy as much space as possible up to the actual regenerator material. During this project several regenerator designs and materials were tested in actual devices including quartz fibers, glass fibers, porous alumina, graphite fibers, and stainless steel fibers.

The final modeling designs indicated that we could only achieve limited amounts of cooling with a limited volume regenerator as shown in Figure 6. In this design, there is a recess in the regenerator face that closely matches the deflection of the diamond diaphragm. The recess forces all of the working fluid through a small volume of actual regenerator material. The area outside of the regenerator region is evacuated to further improve the thermal isolation between the cold and hot faces of the working device. The canister is packed with 4 mm diameter stainless steel fibers provided by Bekaert. An actual regenerator is also shown in Figure 6 with its attached vacuum port. The regenerator is composed of the thin stainless steel and titanium parts previously described in Figure 1. All the parts were assembled using a low vapor pressure epoxy (Torr Seal, Varian and Associates).

### Evacuation and Pressurization Ports

According to our device models, not only must most of the inactive parts of the regenerator have a very low thermal conductivity (most easily achieved by pulling a vacuum between the back-

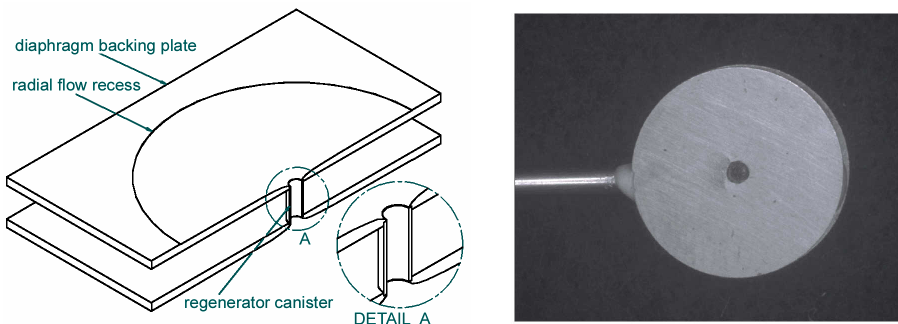


**Figure 6.** The reduced volume regenerator. This regenerator is constructed of stainless steel and/or titanium parts and evacuated between the backing plates.



ing plates outside of the regenerator), but the active parts of the device must be pressurized to at least 500 kPa and most preferably to 1 MPa. The burst point of the 30 mm diamond diaphragms limited the actual pressurization to 600 kPa. The port shown previously in Figure 6 allows for a 10 mTorr. vacuum to be pulled between the backing plates. A similar port was placed between the regenerator and one of the endplate assemblies to allow for pressurization with a working fluid such as He or another inert gas. This port was comprised of a 35 gauge stainless steel tube extending into the active area of the device. In order to easily attach the device to a gas cylinder, a 17 gauge stainless steel tube was placed over the 35 gauge tube and sealed into place with epoxy.

### Final Assembly

The regenerator, pressurization port, and two endplate assemblies were mounted together using a low thermal conductivity, quick-setting epoxy (Devcon S-209). An example of the diamond-based miniature Stirling cooler is shown in Figure 7.

## TESTING

### Diaphragm Membrane Displacement

Deflection measurements of the piezoelectric crystal-driven diamond diaphragms were made using a Keyence LT-8010 Laser Confocal Displacement System (0.1 mm resolution). For these tests, all assembled endplates were driven with a Wavetek 288 Frequency Generator operating with a sinusoidal wave form at 15 V(peak-to-peak) over a range of 0 to 20 kHz in 100 Hz steps. As can be seen from Figure 8, the maximum deflections can vary greatly; however, a maximum deflection of ~4 microns could always be obtained. Some devices were tested at an amplitude greater than 15 Vp-p, but they tended to fail quickly. Devices tested at frequencies higher than 20 kHz did not show increased deflection. When building a device, diamond endplate assemblies having similar deflection characteristics were paired together.

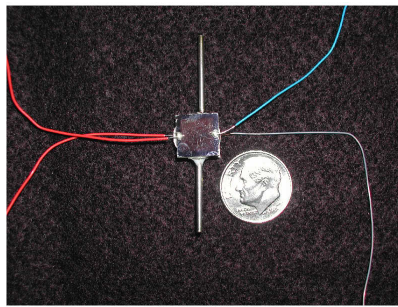


**Figure 7.** Prototype of the diamond-based miniature Stirling cooler.

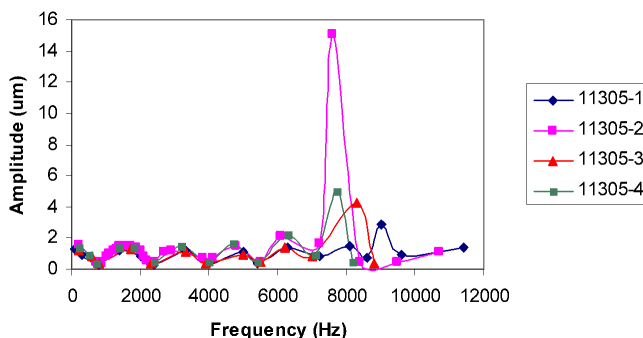


**Figure 8.** Detection of diamond diaphragms driven by thinned piezoelectric crystals. Although large deflections can sometimes be achieved, ~4 micron (maximum) deflections are more common.

To test the maximum displacement that the 30  $\mu\text{m}$  diamond diaphragms could take before failure, a test was devised where a static force was placed on the diaphragm over approximately the same area of the standard piezoelectric drivers. The diaphragm was deflected until the diamond failed as evidenced by a crack or rupture. The diamond diaphragms could typically deflect approximately 50  $\mu\text{m}$  before failure. Thus, the piezoelectric drive system would not initially cause the diaphragms to fail, however, diaphragms with microcracks did fail after several hours of operation due to crack propagation leading to rupture. The more sturdy devices (with no evidence of microcracks) have hundreds of hours of operating time with no evidence of failure.

### Miniature Stirling Cooler Device Testing

Recall that in the Stirling cooling cycle that the hot and cold plate diaphragms must work approximately  $90^\circ$  out of phase with each other. Additionally, the diaphragms must be operating in the fundamental [1,1] mode for square diaphragms if they are expected to produce any real work (basically, a simple trampoline mode). Again using the Keyence LT-8010 and Wavetek 288, the surface of operating diaphragms were mapped out for their deflections. All of the tested diaphragms were found to be operating in the [1,1] mode in a frequency range extending out to 20 kHz.

Testing of the final devices was performed by mounting the coolers on a special jig and introducing the jig into a standard 8" stainless steel vacuum system. The vacuum system performs two duties: 1) it allows for pumping the regenerator's dead volume down to at least 10 mTorr, and 2) it minimizes temperature variations. Type K thermocouple leads are attached to each endplate face to measure temperature differentials between the hot and cold faces. The thermocouple readouts were collected by either a Keithley 195 digital multimeters capable of 100 nV resolution or an Omega DP41-TC high performance temperature indicator with a resolution of 0.01 K. The device to be tested is charged with He to approximately 600 kPa.

An automated test system allowed for testing at various frequencies, amplitudes, operating phases, and integration times while collecting a temperature differential between the hot and cold plates. Again, we were most interested in finding a reversal of the hot to the cold face as we execute a  $180^\circ$  phase change in the operation of the diaphragms. If such a hot-to-cold exchange could be found it would indicate that the Stirling cooler was operating. With our current instrumentation, it is believed that any pumping resulting in a differential temperature would have been observed at a level of at least  $0.1^\circ\text{C}$ .

Although there appears to be some limited amount of cooling at  $\sim 4\text{ kHz}$  in the example shown in Figure 9, a thorough comparison of the data provided no evidence of differential temperatures.

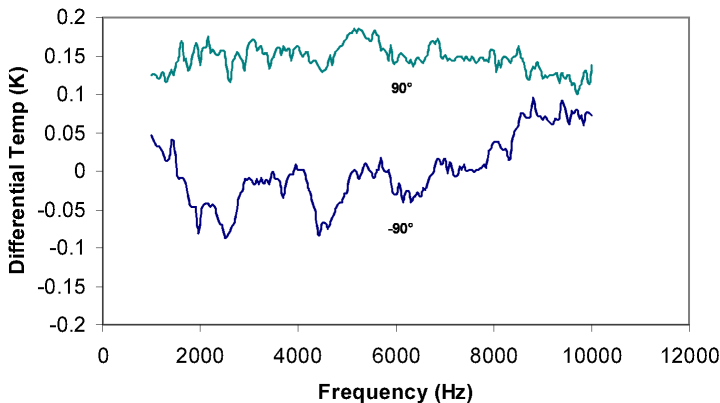


**Figure 9.** Raw data illustrating the differential temperature as a function of frequency and phase shift. This data was taken every 30 seconds at 50 Hz intervals with the phase angles referring to the Stirling cycle phase difference between the operating diaphragms. The temperature variations throughout this study were less than 1 K.



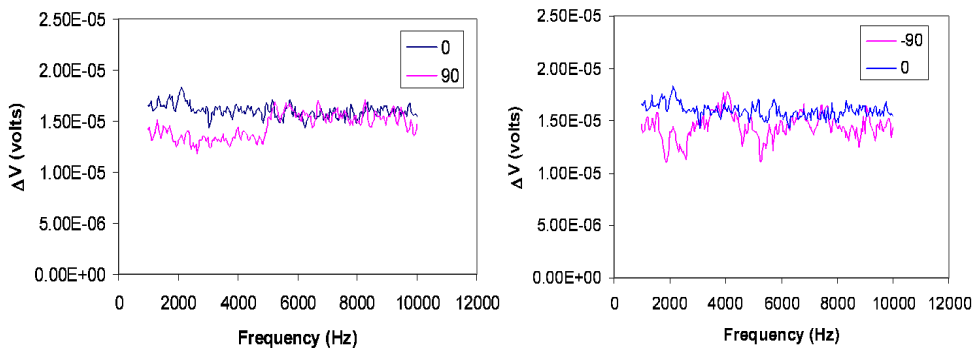


**Figure 10.** Phase dependence on the temperature differential (measured in  $\Delta V$  from thermocouples) for a typical device. There is no switching of the 90 and -90  $\Delta V$  associated with the actual cooling.

Examples of the phase comparisons are shown in Figure 10. The zero phase shift data was compared to all of the other phase shift data with similar results. We also found that slight changes in environmental factors could affect the results, so devices were run at various times of the day in order to normalize all data. The lack of any measurable heat pumping perhaps supplies one more data point for modeling these devices.

## CONCLUSIONS

Several different types of miniature diamond-based cryocoolers were modeled, designed, and built during this SBIR Phase II project. Unfortunately, we have not been able to manufacture a MEMS cryocooler that shows any reproducible cooling. Because our design was symmetric, we expected that a working diamond-based MEMS cryocooler would exhibit inversion of the cold and hot faces of the device as the driver operating phase was shifted from  $90^\circ$  to  $-90^\circ$  during the operating Stirling cycle.

In conjunction with construction of our MEMS based cryocoolers we continued to improve the theoretical model of the MEMS based cryocooler. The most recent models indicate that parasitic heat losses can quickly overwhelm the cooling capability of any refrigerator in our size range ( $\sim 10 \text{ mm} \times 10 \text{ mm} \times 2 \text{ mm}$ ). If a miniature cooler could be built to the extremely tight tolerances suggested by the current models, we would expect a lift of 68 mW between 300 and 280 K.

While we were not able to manufacture a working miniature Stirling cooler, we did design and test a number of components that will enable future devices to work if the design tolerances of the current models can be met. Key components that were built and tested include: a CVD diamond heat exchange plates, a piezoelectric crystal driven diamond diaphragm, and a reduced volume, evacuated regenerator. The diamond endplates and diaphragms have a high thermal conductivity ( $>900 \text{ W m}^{-1} \text{ K}^{-1}$ ) that allow for rapid heat transfer into and out of the cooler. The diaphragms have a measured stroke of approximately 5 mm and can be operated at frequencies in excess of 10 kHz. Larger strokes and higher frequencies lead to rapid failure of the diaphragms. An obvious improvement for future devices is to increase the stroke of the diaphragm via design, material, and driver changes. The regenerator is composed of materials that have a low thermal conductivity and high heat capacity to provide for efficient conduction and storage of heat in the regenerator. The prototype devices are also capable of being charged with a working gas to internal pressures greater than 500 kPa (another necessary component for a working miniature Stirling cooler). Although a working miniature Stirling cooler was not fabricated, we were able to provide empirical data that lead to the refinement of several models used in developing these coolers. The small scale of the devices, and, in particular, the proximity of the hot (compression) and cold (expansion) zones may ultimately render these devices ineffective at best. Changes in piston/diaphragm design and poten-

tially the use of new, advanced materials with better thermal and mechanical properties will be required to make these devices viable at this small scale.

## ACKNOWLEDGMENTS

This work was supported by NASA Ames Research Center through the NASA SBIR Program under contract number NNA04CA10C. Acknowledgment is also due to Michael McAleer for his assistance in preparing drawings for this manuscript.

## REFERENCES

1. Stetson, M.B., "Miniature Internal Stirling Cryocooler." US Patent No. 5,056,317, 15 Oct 1991.
2. Bowman, L. and McEntee, J., "Microminiature Stirling Cycle Cryocoolers and Engines," US Patent No. 5,547,956, 17 Oct 1995 and continued in part in 5,749,226 (12 Mar 1998) and 5,941,079 (24 Aug 1999).
3. Moran, M.E., "Micro-Scalable Thermal Control Device," US Patent No. 6,385,973 B1, 14 May 2002.
4. Erbay, L. B., and Yavuz, H., "The Maximum Cooling Density of a Realistic Stirling Refrigerator", *J. Phys. D.* 31, Vol. 291 (1998).
5. F. Sharipova, "Numerical Simulation of Rarified Gas Flow through a Thin Orifice," *J. Fluid. Mech.* 518, Vol. 35 (2004).